

PREPARATION AND CHARACTERIZATION OF HYBRID FILM FROM CELLULOSE AND Fe₃O₄ NANOPARTICLES

LIPING ZHANG, YING GUAN and JUN RAO

School of Forestry and Landscape Architecture, AnHui Agricultural University, Hefei 230036, China

✉ *Corresponding author: Ying Guan, xiaomi1231@163.com*

Received May 17, 2017

This study introduces a facile and green route to fabricate films from bio-based polymers. A hybrid film from cellulose and Fe₃O₄ nanoparticles was successfully prepared *via* regeneration in ILs. The phase, microstructure, morphology and thermal stability of the composite were characterized by X-ray diffraction (XRD), Fourier transform infrared spectrometry (FT-IR), thermo-gravimetric analysis (TGA) and scanning electron microscopy (SEM). The Fe₃O₄ nanoparticles were dispersed on the surface of cellulose and/or in the cellulose matrix. The obtained cellulose/Fe₃O₄ composite film exhibited excellent mechanical performance, due to its high tensile strength (up to 240 MPa) and good thermal stability. Thus, it can be considered a promising material for applications in the semiconductor field.

Keywords: cellulose, Fe₃O₄ nanoparticles, film, ILs

INTRODUCTION

Over the past few decades, the preparation of nanostructured semiconductor materials has attracted considerable research interest, due to their appreciable physical and chemical properties that differ from those of their bulk state.^{1,2} Semiconductors, such as oxides and chalcogenides, exhibit better absorption in the visible region.³ Iron oxides have been in the focus of scientific investigations due to their natural abundance, stability and easy inter-conversion, which made possible their many applications in technology, *e.g.* in catalysis and magnetic devices.⁴⁻⁷ Iron oxides of both natural and synthetic origin have been used extensively as pigments mainly due to their low price, non-toxicity, opacity and chemical robustness. Recent investigations of iron oxide nanoparticles filled polymers reveal their potential applications in magnetic resonance imaging for molecular diagnosis, targeted drug delivery, hyperthermia anticancer strategy and water treatment.^{8,9}

The growing interest in environmentally friendly materials has promoted research towards the development of biodegradable polymers as an alternative to non-biodegradable synthetic petroleum-derived polymers.^{10,11} In this framework, the aim of this work is to develop a biopolymer-based systems, where sustainable materials would be fabricated solely from renewable feedstocks, which would serve to overcome the depletion of fossil resources. Among environmentally friendly polymers, cellulose, the major structural constituent of the cell walls of plants, is the most abundant natural polymer on earth. It has many advantages, such as superior thermal and mechanical properties, in addition to biocompatibility, biodegradability and cost-effectiveness.^{12,13}

Over the years, cellulose has been used in textiles, furniture and housing. The applications of cellulose have now been extended to high-technology areas, such as biomedical products, bio-energy sources, semiconductor materials and engineered structural reinforcement materials.^{15,16} The dissolution of cellulose is of fundamental importance for its processing and chemical derivatization. Traditional methods used to prepare cellulose materials are often slow; more importantly, they result in serious pollution during the manufacture and post-treatment processes.¹⁴ Also, solvent systems for cellulose dissolution are quite limited because of its high crystallinity associated with extensive hydrogen bonding networks. Over the past decade, ionic liquids (ILs), which are low melting-point salts that form liquids at temperatures below the boiling point of water, have been identified as good solvents for polysaccharides, such as cellulose and chitin.¹⁷⁻²² Swatloski *et al.*²³ pioneered the dissolution of cellulose in 1-butyl-3-methylimidazolium chloride (BMIMCl). This dissolution system provided processing advantages, namely high solubility at a suitable temperature, solubility of 10 wt%

at 100 °C without derivatization and less chain degradation.²⁵ Ionic liquids have many advantages compared with traditional organic solvents, namely, excellent dissolving capability, negligible vapor pressure, ease of recycling and high thermal stability.²⁵⁻²⁷

In this study, we report the fabrication of cellulose films by means of the regeneration technique from ionic liquids from poplar pulp and Fe₃O₄ nanoparticles. The structure of original cellulose and Fe₃O₄ nanoparticles was characterized by FT-IR spectroscopy. The morphology and mechanical properties of the resulting films were evaluated by SEM analysis and tensile testing, respectively. Various films with different proportions of cellulose and Fe₃O₄ nanoparticles were investigated by FT-IR, XRD, TGA and tensile testing. The present approach provides a facile procedure for producing new cellulose-based film materials.

EXPERIMENTAL

Materials

Cellulose was obtained by the alkaline pulping (AP) method from poplar pulp. The mixture of pulp, sodium chlorite, acetic acid and distilled water in the ratio of 1:0.75:0.5:65 was reacted at 75 °C for 1 h. The obtained pulp was washed with distilled water several times to neutral pH and then dried in a vacuum oven at 40 °C for 24 h. The viscosity of the obtained pulp was 1038 g/ml. The ionic liquid was BMIMCl (99.9%), from Lanzhou Institute of Chemical Physics, with a molecular weight of 174.67. The size of the Fe₃O₄ nanoparticles was 20-30 nm. All the chemical materials and solvents used in the experiments were analytical grade reagents and were used without further purification.

Fabrication of cellulose/Fe₃O₄ composite films

In a typical experiment, the obtained cellulose (0.5 g) was dissolved in BMIMCl in a flask under magnetic stirring at 115 °C for 30 min. Then, different contents of Fe₃O₄ nanoparticles were added into the above solution. The mixture was frozen, ball-milled and stirred at 80 °C for 30 min. The temperature was then raised to 115 °C for the mixture to dissolve. Then, the solution was cast on a glass mould for air-drying. Finally, the film was regenerated in distilled water. The films were obtained by drying in a vacuum oven at 40 °C for 24 h. The different reaction conditions of cellulose/Fe₃O₄ composite films were shown and labeled in Table 1.

Table 1
Experimental conditions for preparing the films

Number	Cellulose (g)	Fe ₃ O ₄ /cellulose (w/w)
F0	0.5	0
F1	0.5	0.1
F2	0.5	1.0
F3	0.5	3.0
F4	0.5	5.0

FT-IR analysis

FT-IR spectra of the samples were recorded using a Thermo Scientific Nicolet NEXUS-870 FT-IR Microscope (Thermo Nicolet Corporation, Madison, WI) equipped with a liquid nitrogen cooled MCT detector. Dried samples were ground and palletized using BaF₂ and their spectra were recorded from 4000 to 400 cm⁻¹ at a resolution of 4 cm⁻¹, with 128 scans per sample.

Scanning electron microscopy

SEM of the film samples was carried out with a Hitachi S-4800 (Hitachi, Japan) instrument at 15 kV. Prior to taking pictures, the samples were sputter-coated with a thin layer of gold. Images were obtained at magnifications ranging from 200× to 5000×, which was dependent on the feature to be traced.

X-ray diffraction

The crystallinity of the films was measured using an XRD-2 instrument with a CuKα radiation source ($\lambda = 0.154$ nm) at 40 KV and 30 mA. Samples were scanned from 5° to 40° (2θ) at a speed of 0.5° min⁻¹.

Thermal property of films

Thermal analysis was performed on a simultaneous thermal analyzer (TG209 TG/DTA, Netzsch). The

apparatus was continually flushed with nitrogen. The sample weighing between 9 and 11 mg was heated from room temperature to 700 °C at a heating rate of 10 °C min⁻¹.

Tensile strength

The tensile strength of the films was tested using a universal tensile tester (AG-X-plus, Shimadzu Corporation, Japan) at room temperature. The film samples were 25 mm × 10 mm in dimension (length × width) and a tensile speed of 5 mm min⁻¹ was employed for the tests.

RESULTS AND DISCUSSION

Structure of cellulose/Fe₃O₄ composite films

FT-IR spectroscopy was used to characterize the molecular interaction between cellulose and Fe₃O₄. Figure 1 shows the FTIR spectra of the cellulose fibers and Fe₃O₄ nanoparticles. The typical characteristic bands of cellulose in all the samples at 3400 cm⁻¹ (stretching vibration of OH), 2900 cm⁻¹ (asymmetrical stretching vibration of C-H), 1650 cm⁻¹ (bending mode of adsorbed water), 1435 cm⁻¹ (CH₂ scissoring motion), 1063 cm⁻¹ (C-O in cellulose)²⁸ were observed. In the spectrum of Fe₃O₄, a broad band at 3400 cm⁻¹ and a weak peak at 1500 cm⁻¹ could be seen, which were due to the stretching vibration of OH and Fe-O, respectively.

The five cellulose-based films were further examined by FTIR analysis, as shown in Figure 2. The characteristic absorption bands of cellulose and Fe₃O₄ nanoparticles were all present in the spectra of the five films. The spectrum of the cellulose film was almost identical with those of F1, F2 and F3. However, the absorption bands were influenced by the content of Fe₃O₄ nanoparticles. In the spectrum of F4, the band at 3400 cm⁻¹ was broader than in other spectra, which might be due to the formation of new O-H from the oxygen atom of Fe₃O₄ nanoparticles and the hydrogen atom of cellulose. The frequency of the vibrational band at 1000 cm⁻¹ originating from C-O stretching became weaker, which was due to the formation of the Fe-O bond between Fe₃O₄ nanoparticles and cellulose. This result suggested that the Fe₃O₄ nanoparticles were compounded with cellulose successfully. The stability of Fe₃O₄ nanoparticles in cellulose fibers is very important for the properties of the composite fibers.

The XRD patterns for Fe₃O₄ nanoparticles, cellulose film and four cellulose/Fe₃O₄ composite films are shown in Figure 3. The presence of oxide nanoparticles in some membranes was confirmed by the diffraction peaks at 2θ angles of 29.2° and 35.7°, which correspond to the (220) and (311) crystalline planes of Fe₃O₄ nanoparticles.²⁹ The cellulose film exhibited only one peak at a 2θ angle of 20.0°, assigned to the (110) and (200) plane of crystalline cellulose II.³⁰

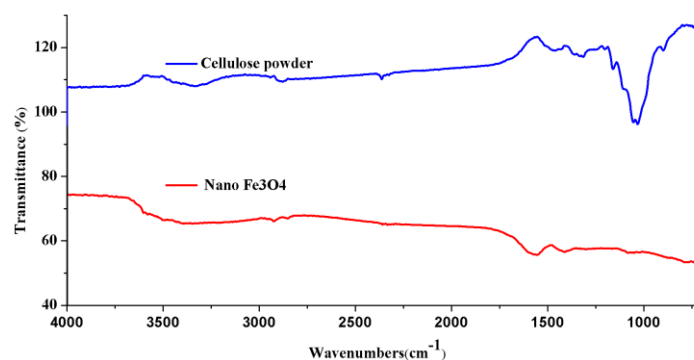


Figure 1: FT-IR spectra of cellulose and Fe₃O₄ nanoparticles

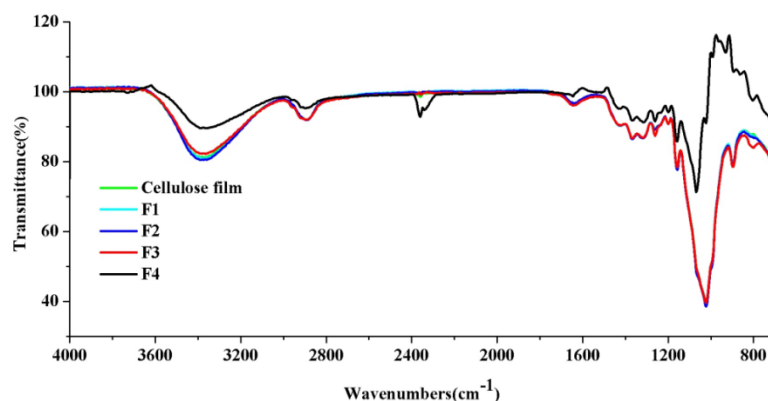


Figure 2: FT-IR spectra of the five films

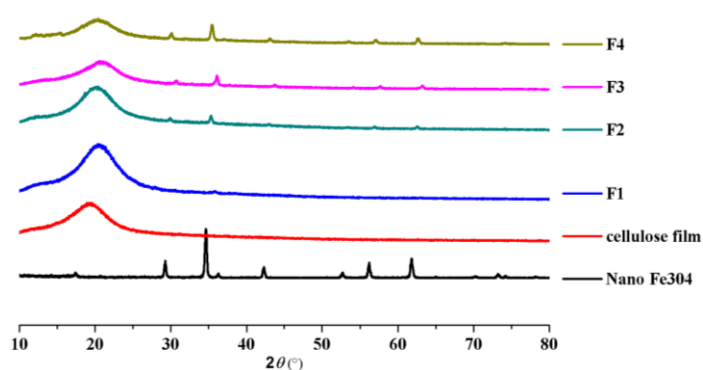


Figure 3: X-ray diffraction patterns of Fe_3O_4 nanoparticles, the cellulose film and four composite films

It may be noted that from Figure 3 that the characteristic peaks of the four cellulose/ Fe_3O_4 composite films with different Fe_3O_4 nanoparticles proportions exhibited different intensities. The reason for not detecting Fe_3O_4 nanoparticles in the spectrum of F1 may be that the integrated Fe_3O_4 quantity was below the detection sensibility of the diffractometer. With the increment of the Fe_3O_4 nanoparticles concentration, the intensity of the diffraction peaks at 2θ angles of 29.2° and 35.7° from Fe_3O_4 nanoparticles increased. The loads of Fe_3O_4 did not produce appreciable changes in the crystalline domains for films. The probable reason for that resides in the fact that the nanoparticles were mainly adsorbed on the fiber surface rather than were encapsulated by it.

Morphologies of cellulose/ Fe_3O_4 composite films

The morphology of the films was further investigated by SEM. It could be seen from Figure 4A that the cellulose film presented homogeneous and smooth surface. This image suggests that the structure of the composite film was improved by regeneration in the IL. In the microstructure of F3 and F4 in Figure 4B and 4C, irregular polygon shapes can be noted, indicating the existence of Fe_3O_4 nanoparticles in the composite matrix of the film. With the increment of Fe_3O_4 nanoparticles concentration, the shape of the Fe_3O_4 nanoparticles became more regular in the composite matrix. The pictures of F4 show that the Fe_3O_4 nanoparticles were nearly cube-shaped and monodispersed. The results indicated that the Fe_3O_4 nanoparticles were compounded with cellulose successfully and the composite films were obtained.

Thermal properties of cellulose/ Fe_3O_4 composite films

TGA is a powerful technique to determine the state of polymers and to evaluate the intermolecular interaction in the composite film matrix. The TGA thermograms of the cellulose film, F1, F2, F3 and F4 are shown in Figure 5. The curves of the five samples with several weight loss steps indicated the influence of different parameters on the degradation of films, such as water evaporation and film degradation. The weight loss below 100°C was mostly attributed to the release of moisture from the

samples. As can be seen from the TGA curves, when the temperature reached 700 °C, the remaining solid residues were in the range of 20-25% for the five films. The TGA curves and the mass loss trends of the five films were absolutely identical. The maximum remaining solid residues of the films was 24.5% for F4, when the minimum was 20.8% for the cellulose film. These results indicated that the thermal stability of the films was improved with the addition of the Fe₃O₄ nanoparticles.

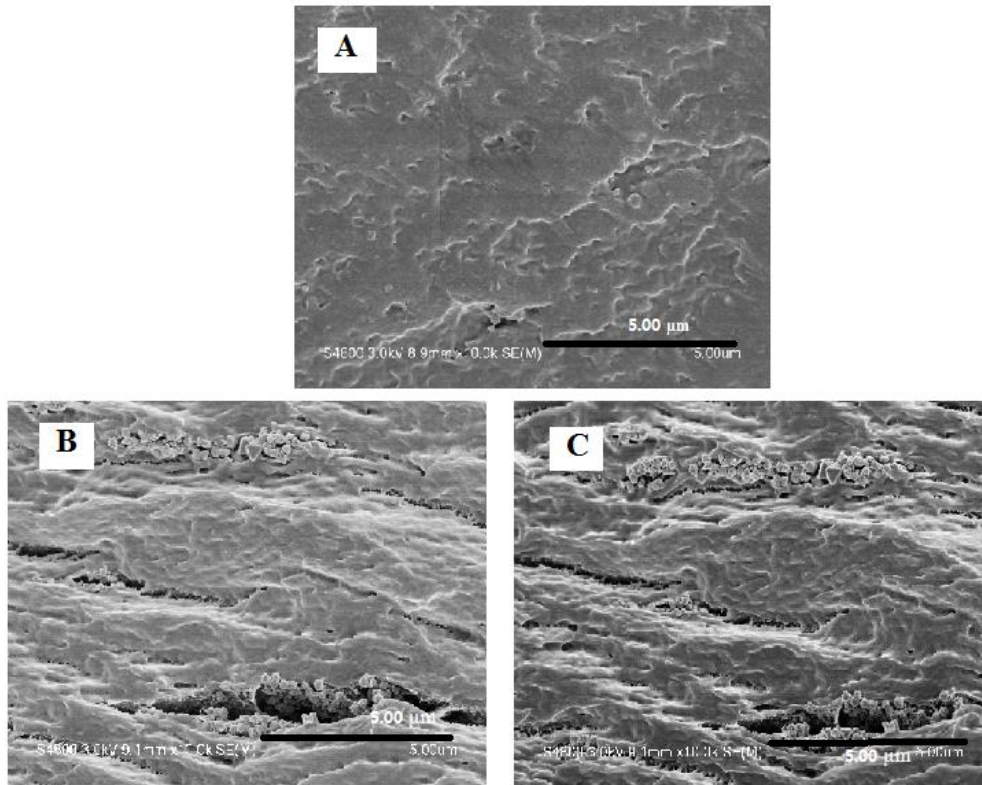


Figure 4: SEM images of cellulose film (A), F3 (B) and F4 (C)

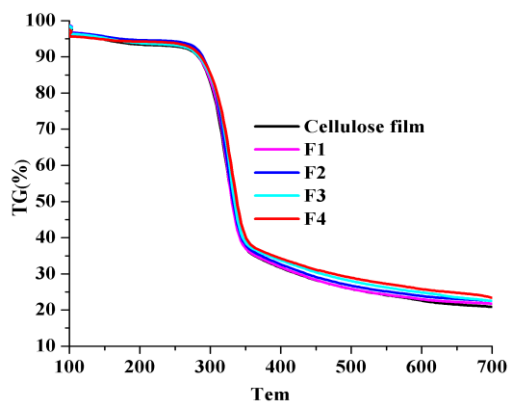


Figure 5: TGA curves of the five films

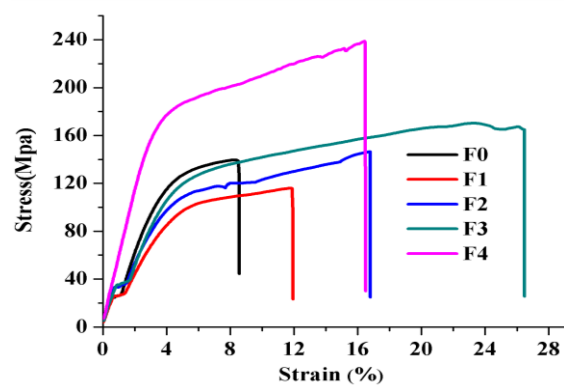


Figure 6: Tensile stress-strain curves for F0-F4

Mechanical properties of cellulose/Fe₃O₄ composite films

The mechanical properties of the films are an important factor, which affects their actual applications. Figure 6 displays the strain-stress curves of the cellulose/Fe₃O₄ composite films in tensile testing. Apparently, the tensile strengths of the films increased with the increment in the concentration of Fe₃O₄ nanoparticles. The tensile strengths of the cellulose films between F2 and F3 were of about 140 MPa. Among the five films, the maximum stress of 240 MPa was reached by F4, which was obtained with 5% concentration of Fe₃O₄ nanoparticles. It suggested that the mechanical strength of

the films was related to the concentration of Fe₃O₄ nanoparticles. Meanwhile, the tensile strains of the films increased with the increment of Fe₃O₄ nanoparticles concentration from F1 to F3. However, when the concentration of Fe₃O₄ nanoparticles was up to 5% (F4), the tensile strain decreased. This indicates that better ductility of the films can be obtained at low concentrations of Fe₃O₄ nanoparticles. Generally, all these films possessed high tensile strength, which enables their wide application.

CONCLUSION

In the present paper, we report an efficient and facile route for the synthesis of cellulose-based composites. Five films with different Fe₃O₄ content were prepared and their properties were investigated. It was found that the concentration of Fe₃O₄ nanoparticles played an important role in the phase and properties of the composite films. The films exhibited uniform structure, good thermal stability and excellent mechanical strength. FT-IR analysis indicated that the Fe₃O₄ nanoparticles were compounded with cellulose successfully. From the results of tensile testing it was noted that the tensile stress of the films increased with increasing Fe₃O₄ content. However, the tensile stress of F4 decreased when the Fe₃O₄ content reached 5.0. This study provides a controllable way to fabricate cellulose-based films, which could greatly extend the application potential of natural polymer films in the field of semiconductors.

ACKNOWLEDGEMENT: This work was supported by Youth Funds of Anhui Agricultural University (2015ZD09), Introduction and Stability Talent Project of Anhui Agricultural University (yj2016-10).

REFERENCES

- ¹ A. P. Alivisatos, *Science*, **27**, 1933 (1996).
- ² V. L. Colvin, M. C. Schlamp and A. P. Alivisatos, *Nature*, **370**, 354 (1994).
- ³ M. Hassan, E. Haque, K. R. Reddy, A. I. Mineett, J. Chen *et al.*, *Nanoscale*, **6**, 11988 (2014).
- ⁴ M. Sugimoto, *J. Am. Ceram. Soc.*, **82**, 269 (1999).
- ⁵ D. S. Mathew and R. S. Juang, *Chem. Eng. J.*, **129**, 51 (2007).
- ⁶ Q. A. Pankhurst, J. Connolly, S. Jones and J. Dobson, *J. Phys. D. Appl. Phys.*, **36**, 167 (2003).
- ⁷ R. M. Cornell and U. Schwertmann, "The Iron Oxides", Wiley-VCH Verlag GmbH & Co. KGaA, 2004.
- ⁸ B. Bonnemain, *J. Drug Target.*, **6**, 167 (1998).
- ⁹ S. Mornet, S. Vasseur, F. Grasset and E. Duguet, *J. Mater. Chem.*, **14**, 2161 (2004).
- ¹⁰ I. Armentano, M. Dottori, E. Fortunati, S. Mattioli and J. M. Kenny, *Polym. Degrad. Stabil.*, **95**, 2126 (2010).
- ¹¹ E. Fortunati, M. Peltzer, I. Armentano, A. Jiménez and J. M. Kenny, *J. Food Eng.*, **118**, 117 (2013).
- ¹² D. Klemm, B. Heublein, H. P. Fink and A. Bohn, *Angew. Chem. Inter. Ed.*, **44**, 3358 (2005).
- ¹³ J. L. Wertz, O. Bedue and J. P. Mercier, "Cellulose Science and Technology", Lausanne, Switzerland, EPFL Press, 2010.
- ¹⁴ J. Cai and L. Zhang, *Macromol. Biosci.*, **5**, 539 (2005).
- ¹⁵ Y. Ahn, S. H. Lee, H. J. Kim, Y. H. Yang, J. H. Hong *et al.*, *Carbohydr. Polym.*, **88**, 395 (2012).
- ¹⁶ R. J. Moon, A. Martini, J. Nairn, J. Simonsen and J. Youngblood, *Chem. Soc. Rev.*, **40**, 3941 (2011).
- ¹⁷ A. Pinkert, K. N. Marsh, S. Pang and M. P. Staiger, *Chem. Rev.*, **109**, 6712 (2009).
- ¹⁸ M. E. Zakrzewska, E. B. Lukasik and R. B. Lukasik, *Energ. Fuels*, **24**, 737 (2010).
- ¹⁹ W. T. Wang, J. Zhu, X. L. Wang, Y. Huang and Y. Z. Wang, *J. Macromol. Sci. B Phys.*, **49**, 528 (2010).
- ²⁰ R. A. A. Muzzarelli, *Mar. Drugs*, **9**, 1510 (2011).
- ²¹ M. M. Jaworska, T. Kozlecki and A. Gorak, *J. Polym. Eng.*, **32**, 67 (2012).
- ²² A. M. Bochek, A. A. Murav'ev, N. P. Novoselov, M. Zaborski, N. M. Zabivalova *et al.*, *Russ. J. Appl. Chem.*, **85**, 1718 (2012).
- ²³ R. P. Swatloski, S. K. Spear, J. D. Holbrey and R. D. Rogers, *J. Amer. Chem. Soc.*, **124**, 4974 (2002).
- ²⁴ N. P. Novoselov, E. S. Sashina, O. G. Kuz'mina and S. V. Troshenkova, *Russ. J. Gen. Chem.*, **77**, 1395 (2007).
- ²⁵ R. C. Remsing, R. P. Swatloski, R. D. Rogers and G. Moyna, *Chem. Commun.*, **12**, 1271 (2006).
- ²⁶ M. B. Turner, S. K. Spear, J. D. Holbrey and R. D. Rogers, *Biomacromolecules*, **5**, 1379 (2004).
- ²⁷ M. B. Turner, S. K. Spear, J. G. Huddleston, J. D. Holbrey and R. D. Rogers, *Green Chem.*, **5**, 443 (2003).
- ²⁸ R. G. Zhibankov, S. P. Firsov and D. K. Buslov, *J. Mol. Struct.*, **614**, 117. (2002).
- ²⁹ J. Sun, S. B. Zhou, P. Hou, Y. Yang, J. Weng *et al.*, *J. Biomed. Mater. Res. A*, **80**, 333 (2007).
- ³⁰ T. Nishino, K. Takano and K. Nakamae, *J. Polym. Sci. B: Polym. Phys.*, **33**, 1647 (1997).